




## Article

# A Novel Method of Local Anode Effect Prediction for Large Aluminum Reduction Cell

Jiarui Cui <sup>1,3,\*</sup> , Zhijing Li <sup>1</sup>, Xiangquan Li <sup>2</sup> , Bo Liu <sup>2</sup>, Qing Li <sup>1,\*</sup> , Qun Yan <sup>1</sup>, Ruoyu Huang <sup>3</sup>, Hui Lu <sup>3,\*</sup> and Bin Cao <sup>3</sup>

<sup>1</sup> School of Automation and Electrical Engineering, University of Science and Technology Beijing, Beijing 100083, China

<sup>2</sup> School of Information Engineering, Jingdezhen University, Jingdezhen 333000, China

<sup>3</sup> Guiyang Aluminum Magnesium Design and Research Institute Co., Ltd., Guiyang 550081, China

\* Correspondence: cuijiarui@ustb.edu.cn (J.C.); liqing@ies.ustb.edu.cn (Q.L.); hui\_lu@chalieco.com.cn (H.L.)

**Featured Application:** Local anode effects occur more frequently in large-scale aluminum electrolysis cell systems. But the existing equipment can only detect global anode effects, which resulting in instability and high energy consumption in the aluminum electrolysis production process. This work is mainly used in the prediction of local anode effect. Through the prediction of anode effect, manual intervention can be carried out in advance, which can effectively avoid the occurrence of unnecessary anode effect, thereby improving the stability of the production system and reducing the DC power consumption of the system.

**Abstract:** A method of local anode effect prediction is proposed for the problem that it is difficult to detect the local anode effect in large aluminum reduction cell in real time. Firstly, a fuzzy classification of local anode effect prediction in terms of fuzziness level is proposed considering various working conditions of anode current in the region. Secondly, a current volatility detection method based on time-sliding window density is designed from the problem of uneven current distribution in the region, and the anode currents in the region are classified and tracked for prediction according to the different current volatility. Thirdly, an improved Gated Recurrent Unit (GRU) neural network structure is proposed to improve the prediction accuracy of fluctuating currents. Finally, simulation experiments are conducted based on actual data, and compared with Long Short-Term Memory (LSTM) and Convolutional Neural Network-Long Short-Term Memory (CNN-LSTM), the proposed method has certain advantages in both prediction time, training time, and the mean absolute error (MAE) and mean square error (MSE), which verifies the effectiveness of the proposed method.

**Keywords:** aluminum electrolysis; local anode effect prediction; neural network; time series tracking prediction



**Citation:** Cui, J.; Li, Z.; Li, X.; Liu, B.; Li, Q.; Yan, Q.; Huang, R.; Lu, H.; Cao, B. A Novel Method of Local Anode Effect Prediction for Large Aluminum Reduction Cell. *Appl. Sci.* **2022**, *12*, 12403. <https://doi.org/10.3390/app122312403>

Academic Editors: Jin Guo and Wei Su

Received: 24 October 2022

Accepted: 1 December 2022

Published: 4 December 2022

**Publisher's Note:** MDPI stays neutral with regard to jurisdictional claims in published maps and institutional affiliations.



**Copyright:** © 2022 by the authors. Licensee MDPI, Basel, Switzerland. This article is an open access article distributed under the terms and conditions of the Creative Commons Attribution (CC BY) license (<https://creativecommons.org/licenses/by/4.0/>).

## 1. Introduction

Anode effect prediction is one of the research focuses in the production of modern aluminum electrolysis industry. Anode effect is a special phenomenon in the production process of aluminum electrolysis. If the anode effect occurs in one or some anodes, the voltage and anode current density on these anodes will rise sharply in a short time, resulting in a decrease in the current efficiency and a shortened life of the aluminum electrolytic cell. In addition, the anode effect will produce two kinds of perfluorocarbon gases, CF<sub>4</sub> and C<sub>2</sub>F<sub>6</sub>, with strong greenhouse effect, which have a global warming potential 6630 and 11,100 times higher than that of CO<sub>2</sub> [1]. Therefore, the earlier detection of anode effect for reducing its number has important theoretical value and practical significance.

In the last few years, the research on anode effect mostly focused on the prediction of global anode effect, due to the small scale of aluminum electrolytic cell. The current detecting methods for the occurrence of anode effect is to monitor the changes of cell

voltage and cell resistance. Until now, the direct prediction of anode effect is not realized in industrial production [2]. In literature [3], a model was proposed to extract the fault signatures of anode effect based on the combination of digital filter and local mean decomposition, which lays the foundation for anode effect prediction. Zhou et al. [4] used generalized regression neural network to identify and simulate the cell voltage before and after the anode effect of aluminum electrolytic cell. After training and verifying the model with field data samples, the occurrence of anode effect can be predicted online about half an hour in advance. Yang et al. [5] proposed a robust dictionary learning method, which improved the fault detection rate of anode effect and reduced the false alarm rate. In literature [6], a nonlinear process anode effect monitoring method was proposed based on Kernel dictionary learning algorithm. Chen et al. [7] proposed a data fusion algorithm based on collaborative prediction model to predict the global anode effect by using the similarity search principle. Yin et al. [8] excavated the key feature information of the anode effect by constructing a stacked denoising autoencoder, and sorted the key features by the random forest algorithm to solve the problem of uneven sample distribution in the prediction of the anode effect. At the same time, the Long Short-Term Memory (LSTM) neural network was used to predict the global anode effect. The above research was aimed at the prediction of global anode effect. Due to the violent reaction when the global anode effect occurs, a large number of bubbles overflow, and the slot controller alarms, which is convenient for observation and recording. At present, the study of global anode effect based on data-driven has been relatively mature, and the prediction point of global anode effect can be advanced to about 20 min. Neural network, machine learning, and other methods are used to predict the occurrence of anode effect, which is feasible and accurate.

With the development of computer technology and the improvement of the production process of aluminum electrolytic cell, the aluminum electrolytic cell is gradually developing towards large scale [9], which leads to the difficulty of controlling the production of aluminum electrolysis. In addition, because of the increasing scale of the cell, the key parameters of the aluminum electrolytic cell are unevenly distributed, and the local anode effect happened frequently. The occurrence of local anode effect often precedes the global anode effect. The effective prediction of local anode effect is conducive to preventing the occurrence of global effect. Therefore, with the development of large-scale electrolytic cell, the prediction of local anode effect has gradually become the focus of research. Ding et al. [10] proposed the distribution of alumina concentration in the feeding process based on the finite element mechanism analysis, however the finite element algorithm takes a long time to calculate. So it will take a long time to get the training data, and it is not feasible to predict the anode effect. Wong et al. [11] obtained the influence of fluoride bubbles on the cell voltage by simulating the equivalent circuit of aluminum electrolytic cell, and then predicted the occurrence of local anode effect. By analyzing the distributed anode current, Håkon [12] divided the anode effect into conventional anode effect and low-voltage anode effect according to the cell voltage setting threshold of 8 V. The detection of low-voltage anode effect is analyzed by monitoring the non-uniformity of the current distribution of the anode rod, which proves the feasibility of the distributed anode rod current to predict the anode effect. Aiming at the problem of uneven alumina concentration distribution in large-scale aluminum reduction cells, Zhang et al. [13] proposed the idea of uniform alumina concentration control based on single point feeding and combined with the effect prediction system based on anode current distribution, which greatly reduces the probability of anode effect in the in aluminum reduction cells. By analyzing the power spectrum of the distributed anode rod current, Cui et al. [14] divided the aluminum reduction cell into areas, and determined the occurrence of local anode effect by setting the current fluctuation threshold. Yang et al. [15] developed a low-voltage anode effect prediction method based on the periodic average current deviation ratio by averaging the distributed anode current in time windows, and proposed a multi-point feeding strategy based on the probability distribution of low-voltage anode effects.

Due to the complex on-site environment of high temperature, high magnetism and multi-field coupling in the aluminum electrolysis industry and the complex physicochemical process reaction in the cell, it is difficult to achieve online real-time measurement of alumina concentration, the core parameter that reacts to local anodic effect. While distributed current, as an important parameter affecting the occurrence of anode effect, can be collected in real time. By tracking and predicting the fluctuation of anode current data, the occurrence time and intensity of local anode effect can be effectively predicted, so as to prevent the occurrence of global effect through reasonable and effective measures.

This paper proposes a prediction method of local anode effect of aluminum reduction cell based on distributed current fluctuation detection. Firstly, through the analysis of the aluminum electrolysis production process, a current fluctuation detection method based on the density of the time sliding window is designed to detect the fluctuation of anode current. Secondly, according to the difference of current fluctuation, the anode current in the area is classified and predicted. The Gated Recurrent Unit-Long Short-Term Memory (GRU-LSTM) hybrid neural network is used to track and predict the anode rod current with fluctuation, and the Autoregressive Integrated Moving Average (ARIMA) algorithm is used to track and predict the anode rod current without fluctuation. The occurrence time and intensity of local anode effect are given by combining these two algorithms. Finally, the local anode effect prediction simulation experiment is carried out based on the actual industrial aluminum plant data.

Innovations: (1) The local anode effect is predicted, and the fuzzification level classification of the local anode effect prediction is proposed. (2) A current volatility detection method based on time-sliding window density is designed to classify and track the prediction of anode current in the region according to the current volatility.

## 2. Aluminum Electrolysis Process and Anode Effect Analysis

### 2.1. Aluminum Electrolysis Production Process

The purpose of aluminum electrolysis is to obtain high purity aluminum. In the modern aluminum electrolysis industry, the Hall-Erui method is still the main method due to its wide applicability and ease of operation. Pre-baked aluminum reduction cells are widely used in modern aluminum electrolysis. The structure diagram is shown in Figure 1.

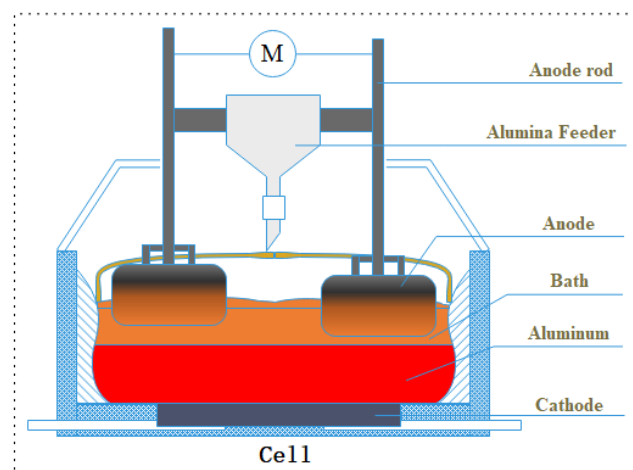


**Figure 1.** Structure diagram of modern aluminum reduction cell.

The entire production process of aluminum electrolysis is carried out in the aluminum electrolytic cell. The raw material for production is aluminum oxide powder, the electrolyte is molten cryolite, and the anode material is carbon. Under the action of high temperature and direct current, reaction occurs in the cell, and aluminum liquid is produced at the cathode. After processing, aluminum liquid is made into various aluminum products.

### 2.2. Analysis of Anode Effect

Anode effect is a special phenomenon when carbon anode is used in molten salt electrolysis. When the concentration of locally dissolved aluminum oxide in the aluminum reduction cell is insufficient (<1%) or the local current density of the anode increases to its critical current density, the anode effect starts on several separate anodes locally and gradually spreads to the whole cell over time [16].

With the development of large-scale aluminum reduction cells, the problem of uneven distribution of parameters gradually appears in aluminum reduction cells. Therefore, the concentration of aluminum oxide is too low in local areas. Then the current of one or two local anodes fluctuates and slowly affects the nearby anodes, after which the anode effect occurs in one or two local anodes, which is called local anode effect. The generation of fluorinated gas makes the contact between several local anodes and the electrolyte worse, thus seriously increasing the local anode resistance. The current is transferred to other anodes of the electrolytic cell, resulting in the increase of current density on other anodes. When the critical current density is exceeded, the anode effect also occurs on other anodes, and the anode effect spreads in the electrolytic cell, eventually leading to the global anode effect [17,18]. Therefore, the local anode effect often precedes the global anode effect. So effective prediction of the local anode effect is conducive to preventing the global anode effect.

### 3. Anode Rod Sequence Fluctuation Detection Algorithm Based on Sliding Window

The current 400 kA aluminum electrolytic cell has six feeding points evenly distributed over the space, and each port has the greatest impact on the nearest surrounding area. In order to reduce the time and computational effort in the process of tracking and predicting the distributed anode current sequence, the 400 kA aluminum electrolytic cell is divided into six areas according to the feeding point, as shown in Figure 2. Each area contains four anode rods on the A side and four on the B side. The current sequence of each area is divided into several window current segments through the sliding window [19], and the current of each sliding window is analyzed to monitor the current fluctuation.

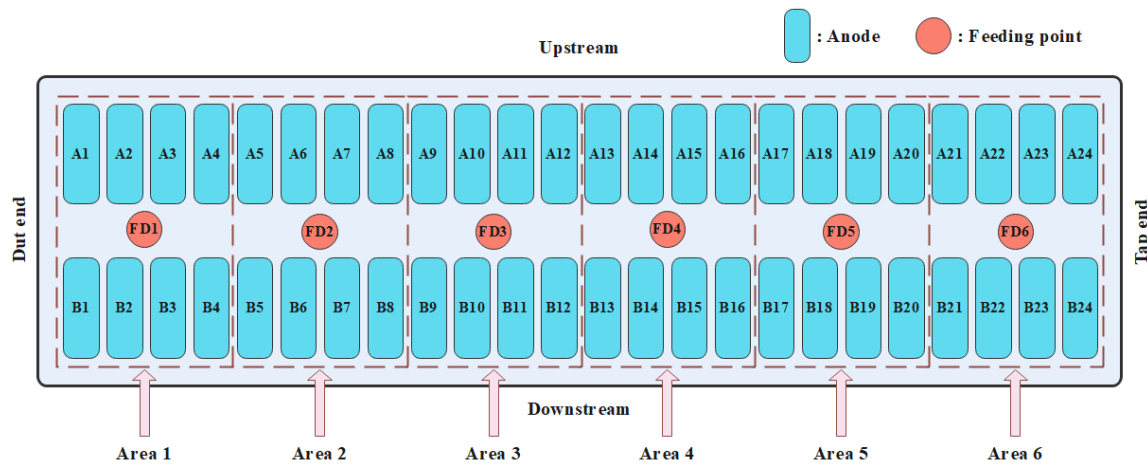


Figure 2. Partition diagram of anode rod of 400 kA aluminum reduction cell.

#### 3.1. Sliding Window Current Series Segmentation

First, current sequence data was segmented by sliding window, and set the current sequence as:

$$I_{anode} = (i(t_1), i(t_2), i(t_3), i(t_4), \dots, i(t_n)) \tag{1}$$

where,  $I_{anode}$  is current data of the acquisition point at each time, and  $t_1 - t_n$  represents the time. In the current sequence, a fixed length sliding window  $m(m \ll n)$  is used for sliding segmentation of the current sequence. The principle is shown in Figure 3. The window

moves backward one step length  $l$  for each sliding, and slides  $(n - m)/l$  times to form  $(n - m)/l + 1$  subsequences.

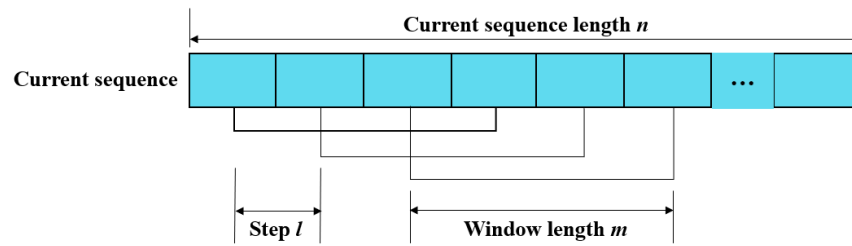


**Figure 3.** Principle of current sequence sliding window.

Assuming one of the subsequences is  $Y_j(1 \leq j \leq (n - m)/l + 1)$ , the slope between any two adjacent data points in the subsequences can be calculated according to Formula (2):

$$k_i = \frac{Y_j(i) - Y_j(i - 1)}{t_i - t_{i-1}}, (2 \leq i \leq m) \tag{2}$$

In this time window  $Y_j$ , there are  $m - 1$  slopes of adjacent current data.  $K_{mean}$  is the average of the current slope of the time window, while  $c$  is the average of the current data within the time window. The window length  $m$ , the average slope value  $K_{mean}$ , and the average value  $c$  form an array  $X_j(m, K_{mean}, c)$ . Then, the current sequence sliding window data is analyzed, and its fluctuation is determined by the standard deviation and the change in the slope of the window data.

### 3.2. Fluctuation Monitoring of Current Sequence

To better monitor the fluctuation of the current sequence, the classification monitoring is performed by setting the distance radius threshold of the slope confidence interval to determine whether the time series produces fluctuations, and let the distance radius  $d_j$  of the slope confidence interval of the  $j$ -th sub-time window current sequence  $Y_j$  be:

$$d_j = \frac{|\bar{\theta}_j - \theta_j|}{2} \tag{3}$$

$$\bar{\theta}_j = \bar{s}_j + \frac{\sigma_j}{\sqrt{l}} Z_{\frac{\alpha}{2}} \tag{4}$$

$$\theta_j = \bar{s}_j - \frac{\sigma_j}{\sqrt{l}} Z_{\frac{\alpha}{2}} \tag{5}$$

where,  $\bar{\theta}_j$  is the upper confidence limit;  $\theta_j$  is the lower confidence limit.  $\bar{s}_j$  is the mean slope of the current sequence of the  $j$ -th sub-time window;  $\sigma_j$  is the mean square deviation of the current sequence slope of the  $j$ -th sub-time window;  $Z$  is the standard normal distribution;  $\alpha$  is the confidence level, which is used to improve or reduce the sensitivity of the confidence interval.

After obtaining its confidence interval radius, the fluctuation threshold is set to  $\beta$  according to the historical current fluctuation. If  $d_j > \beta$ , the current sequence of sub-time window is judged to fluctuate, and the serial number  $j$  of the fluctuating sub-time window is output.

In order to further improve the detection rate, the density difference between the array matrix  $X_i(m, K_{mean}, c)$  and ten adjacent sliding windows (select the first five and the last five of the current windows) is compared. If there are more densities similar to this current sequence, the smaller the probability of its generation fluctuations. The array density

of sliding windows and the distance between different sliding windows are somewhat correlated. For example, the time window object  $X_1$  and  $X_2$  define its distance as:

$$d(X_1, X_2) = \sqrt{\frac{(m_1 - m_2)^2 + (K_{mean1} - K_{mean2})^2 + (c_1 - c_2)^2}{3}} \quad (6)$$

Then the fluctuation monitoring algorithm process is:

STEP1: Select ten sliding windows;

STEP2: For the sliding window, the attainable density  $lrd_k(X)$  is calculated according to Equation (7):

$$lrd_k(X) = \frac{|N_k(X)|}{\sum_{o \in N_k(X)} reachdist(X, o)} \quad (7)$$

where,  $|N_k(X)|$  is the number of sub time series in the neighborhood of the  $k$ -th distance of sub window object  $X$  (expressed as  $k$ -distance( $X$ ), where  $distance(X)$  is calculated by Formula (8)),  $N_k(X)$  is the set of sub-time window objects in the neighborhood of the  $k$ -th distance of sub-time window object  $X$ , and  $o$  is an element of it. The  $k$ -th distance neighborhood is defined as the set of objects whose distance between the selected sample space and object  $X$  is less than or equal to  $k$ -distance( $X$ ).  $reachdist(X, o) = \max\{k$ -distance( $o$ ),  $\|X - o\|\}$  is the maximum value of the  $k$ -th distance of sub-time window  $o$  and the distance between sub-time window object  $o$  and sub-time window object  $X$ .

STEP3: Calculate the ratio  $LOF_k(X_i)$  of the mean value of reachable density of the ten neighboring sub-time-window objects  $X$  to the local reachable density of object  $X_i$  as shown in Formula (8):

$$LOF_k(X_i) = \frac{\frac{1}{|N_k(X_i)|} \sum_{o \in N_k(X_i)} lrd_k(X_i)}{lrd_k(X_i)} \quad (8)$$

STEP4: The calculated results are compared with 1. The closer the reachable density ratio is to 1, the closer the density is, the more stable the current sequence remains; and the greater the calculation result is than 1, the greater the difference between it and the mean of the attainable density of the time window of the nearest neighbor, and the stronger the fluctuation of the current sequence. The current fluctuation intensity can be determined by the parameter  $LOF_k(X_i)$ .

STEP5: Through the comprehensive results of the comparison between the distance radius of the slope confidence interval of the current sequence  $Y_j$  of the sub-time window and the threshold value and the density comparison between the array matrix and the adjacent ten sliding windows (select the first five and the last five of the current windows), it is shown whether current fluctuations occur and the their intensity of current fluctuations.

#### 4. Prediction of Local Anode Effect Based on Analysis of Anode Guide Current Fluctuation

The above method is used to detect the anode current fluctuation in different areas of the aluminum electrolytic cell. If current fluctuation is detected in an anode rod of the electrolytic cell, the current of eight anode rods in the current fluctuation area is tracked and predicted. The anode rods in this area are divided into two groups, non-fluctuation anode rods and fluctuation anode rods, according to the current fluctuation detection results. The ARIMA model is used to track and predict the current of non-fluctuation anode rods in this area, GRU-LSTM hybrid neural network is used to track and predict the current of fluctuating anode rods, and the predicted value  $T_p$  at the moment of anode effect is determined from the current tracking results of fluctuation anode rods, and the local anode effect level is determined according to the number of changes from non-fluctuation anode rods to fluctuation anode rods and violently fluctuating guides predicted by the ARIMA model within  $T_p$ . The flow diagram of local anode effect prediction based on fluctuating anode current detection is shown in Figure 4.



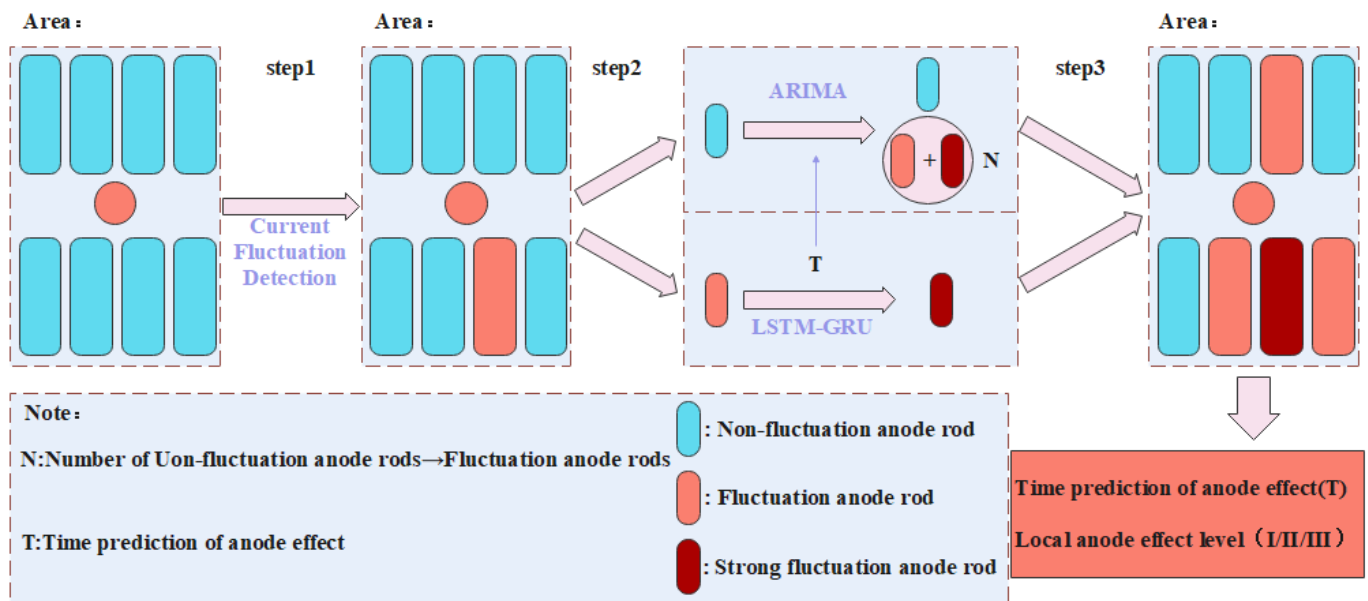


Figure 4. Flow diagram for prediction of local anode effect.

STEP1: The current sequence data of eight anode rods in one of areas is obtained by dividing the areas according to the electrolytic cell structure. The current sequence is divided by a sliding window. The current sequence fluctuation detection algorithm is used to detect its fluctuation and locate the anode rod where the current fluctuation occurs.

STEP2: For the fluctuation detection results in STEP1, the GRU-LSTM hybrid neural network is used to track and predict the current of the fluctuating anode rod in this area, and the predicted value of the strong fluctuation current determines the strong fluctuation occurrence time  $T_p$  (fluctuating anode rod  $\rightarrow$  strong fluctuating anode rod); the AMIRA model is used to track and predict the current of the non-fluctuating anode rod in this area. According to the prediction results, the number  $N$  of the anode rod changing from non-fluctuating to fluctuating and strong fluctuating in  $T_p$  time is determined.

STEP3: The time  $T_p$  in STEP2 is taken as the prediction value of the time when the anode effect occurs, and the local anode effect level is divided according to the number  $N$  of new fluctuation anode rods and strong fluctuation anode rods.

#### 4.1. Prediction of Fluctuating Anode Current Based on GRU-LSTM Hybrid Neural Network

In order to predict the current of the fluctuating anode rod, a new prediction method based on GRU-LSTM hybrid neural network model is proposed. The LSTM and Gated Recurrent Unit (GRU) networks have been widely used in the field of time series detection. They are suitable for tracking and predicting the fluctuating current series and can be used as the prediction model of the fluctuating anode rod current.

The LSTM is a variant of Recurrent Neural Network (RNN) [20] that adds long-term data memory units to the network structure, while setting the gate function to determine the amount of memory and forgetting of historical information. The gated neuron structure is shown in Figure 5. When the neuron is at time  $t$ ,  $h_{t-1}$  is the output of the previous neuron, and  $x_t$  is the input of the neuron at time  $t$ . And  $h_t$  is the output of the neuron. Three gate states are included to determine the memory and forgetting of information.

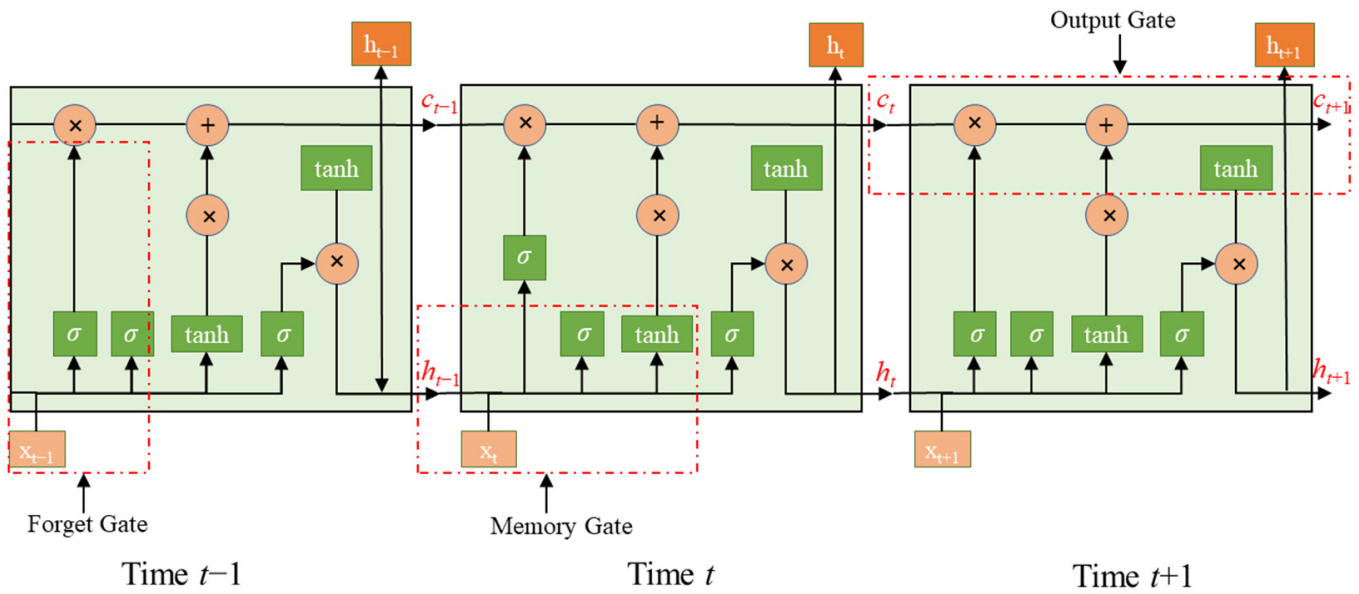


Figure 5. Structure of LSTM gated neurons.

4.1.1. Forget Gate

The forget gate is used to discard the unimportant information in the neuron, and its function realization process is:

The neuron output  $h_{t-1}$  at the  $t - 1$  time and the current time input  $x_t$  are input into the *sigmoid* function, and the activation function will output the weight value (0–1). The output value (0–1) indicates that the state information of the previous neuron has been forgotten to the extent of memory. And 0 means abandoned and 1 means reserved. The output of the forget gate is as shown in Equation (9):

$$f_t = \sigma(W_f[h_{t-1}, x_t] + b_f) \tag{9}$$

where,  $W_f$  is the weight value of the forget gate,  $b_f$  represents the threshold value of the forget gate,  $\sigma$  is the *sigmoid* activation function, and  $[h_{t-1}, x_t]$  is the vector matrix of the neuron state and time at the previous moment.

4.1.2. Memory Gate

$[h_{t-1}, x_t]$  will also be used as input while entering the calculation of the forget gate. The neuron state information at time  $t$  is calculated through the *tanh* activation function, and the information to be updated is obtained by Hadamard product of the neuron state at moment  $t$  with  $i_t$ . As shown in Equation (10) and Equation (11),  $W_i$  and  $W_c$  respectively represent the weight of the memory gate, and  $b_i$ ,  $b_c$  respectively represent the bias of different states of the memory gate.

$$i_t = \sigma(W_i[h_{t-1}, x_t] + b_i) \tag{10}$$

$$c_t = \tanh(W_c[h_{t-1}, x_t] + b_c) \tag{11}$$

GRU is a member of the Recurrent Neural Networks (RNN) family. Compared with LSTM, GRU can also solve the problem of gradient saturation in the memory and back propagation of historical data, which are common in RNN. However, due to its simplified structure, the neuron parameters are much less than LSTM, and only a gated unit is used to perform the operation of forgetting and selective memory of historical data. The structure of gated neuron is shown in Figure 6.



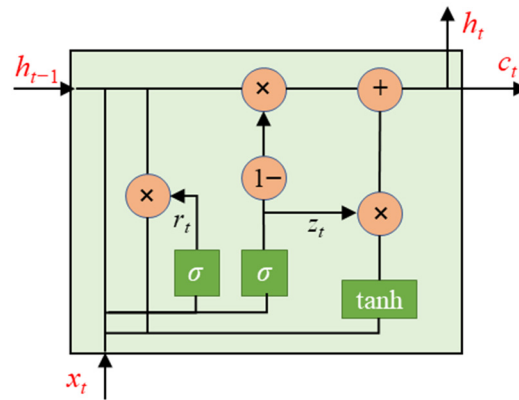


Figure 6. GRU gated neuron structure.

The output of GRU reset data gate and GRU update gate are as follows:

$$r_t = \sigma(W_r[h_{t-1}, x_t] + b_r) \tag{12}$$

$$z_t = \sigma(W_z[h_{t-1}, x_t] + b_z) \tag{13}$$

where,  $r_t$  is the output of GRU reset data gate;  $W_r$  is the weight matrix of reset gate;  $h_{t-1}$ ,  $x_t$  constitute the vector of the neuron hidden layer and the data input layer, which is continuously updated with the input;  $b_r$  is the bias matrix;  $z_t$  is the output of GRU update gate;  $W_z$  is the weight matrix of the update gate. It is calculated by *sigmoid* function to narrow the output values to (0–1).

$$h_t' = \tanh(W_h[r_t \odot h_{t-1}, x_t] + b_h) \tag{14}$$

where,  $h_t'$  is the neuronal state at time  $t$ ;  $W_h$  is the weight update matrix of neuronal state;  $\odot$  is Hadamard product;  $b_h$  is the bias matrix of neuronal state; the neuronal state is limited to (–1,1) by hyperbolic tangent function.

$$h_i = z_i \odot h_{i-1} + (1 - z_i) \odot h_i' \tag{15}$$

where,  $h_t'$  is calculated by Equation (14). As can be seen from the above formula, the output of the update gate strictly controls the retention or not of the information flow of the previous state in the neuron, with  $z_i$  varying between (0–1) [21], to ensure that the control output is the ratio of the state of the unit at the previous moment to the unit input being input, to achieve the memory of important information, forgetting the inputs that have less impact on the neuron unit, and to constantly update the parameter architecture of the neuron hidden layer.

Since the training time of LSTM network is slightly longer, in order to improve the training speed of neural network and realize online current tracking, the advantages of LSTM and GRU networks are combined, and LSTM and GRU are combined by full link to form a current prediction model to achieve fast current tracking and high accuracy at the same time. The occurrence point of strong fluctuation of anode current can be determined in advance by current tracking, which can be used as the prediction value of the occurrence time of anode effect.

It is defined that the strong fluctuation current value of anode current is equal to or greater than 1.5 times of the average value of 20 current sampling values before the fluctuation [22]:

$$I_{ts} \geq 1.5 \times \frac{\sum_{t=tp-20}^{tp} I_t}{20} \tag{16}$$

where:  $tp$  is the time point when strong current fluctuation is detected, and  $I_{ts}$  is the strong current fluctuation value;  $I_t$  is the current sampling value.

According to (16) the current data before the time point when the strong fluctuation current  $I_{ts}$  of the anode is detected in advance is input into the GRU-LSTM hybrid neural network for training and learning. The GRU-LSTM hybrid neural network after training is used to track and predict the anode rod that has fluctuated, and the value of strong fluctuation current  $I_{ts}$  and the time of strong fluctuation  $tp$  are obtained as the predicted value of the time when the anode effect occurs.

#### 4.2. Tracking Prediction of Non-Fluctuating Anode Current Based on ARIMA Model

The local anode effect occurs 5–15 min before the current fluctuation of one or several guide rods. But under the working condition that the local alumina concentration of the contact part between the anode rod and the electrolyte decreases (according to expert experience [16], when the aluminum concentration is lower than 1.5%, the electrolyte balance will be broken, and the anode effect is early to occur), it takes some time to spread to other nearby anode rods. So tracking the current changes of other anode rods in the same area that have not yet fluctuated will provide an important reference for anode effect prediction.

The differential ARIMA model is an algorithm for forecasting short-term, medium, and long-term time series information [23].  $ARIMA(p, d, q)$  model is essentially a combination of difference operation and  $ARIMA(p, q)$  model. The basic process is as follows: first, the obtained time series data are checked for stationarity, and then the non-stationary time series data is converted into the stationary time series data by the  $d$ -difference operation; then, the order of stationary time series data are determined and the parameters are estimated to obtain the values of  $p, q$ ; finally,  $ARIMA(p, q)$  model is used to predict the time series.

Considering the algorithm computation, operability, real-time and other factors, if the anode rod current is detected to fluctuate, the ARIMA model is used to track and predict the current of the anode guide rods that do not fluctuate in the area where the anode rods are located. First, the stationary data is obtained by performing  $d$ -difference operation on the obtained time series current; after that, the  $ARIMA(p, q)$  is fitted to a fixed order to determine the  $p$  and  $q$  parameters; then, the ARMA model is used to track the current sequence of the anode rod without fluctuation and output the current prediction value for a certain time in the future. If the error between the current prediction value and the actual current is greater than the set threshold value, it is considered that the current of the anode rod tracked has fluctuated; finally, the local anode effect level is determined according to the number of non-fluctuating anode rods changing into fluctuating anode rods in this area.

The ARMA model of the original anode rod current after stationarity treatment is as follows:

$$I_t = \varphi_1 I_{t-1} + \varphi_2 I_{t-2} + \cdots + \varphi_p I_{t-p} + \varepsilon_t - \theta_1 \varepsilon_{t-1} - \cdots - \theta_q \varepsilon_{t-q} \quad (17)$$

where,  $I_t$  is the original anode rod current signal;  $p, q$  is the order of ARMA model, which is determined by the autocorrelation coefficient and partial correlation function of the sequence;  $\varphi_p, \theta_q$  are the model coefficient;  $\varepsilon_t$  is the mean square error of the current sequence.

#### 4.3. Local Anode Effect Level Strategy

According to the current prediction results of the non-fluctuated anode rods by (17) and the current prediction results of the fluctuated anode rods by the GRU-LSTM hybrid neural network, the prediction results of the local anode effect are jointly determined. At the same time, in order to reduce the false alarm rate, the local anode effect level is fuzzified and divided into three levels: I, II and III, which respectively represent that:

I: the current prediction value of fluctuating anode rod is greater than the set threshold, and the predicted value of non-fluctuating anode rod current is less than the set threshold  $\alpha$ ;

II: The predicted value of the current of the fluctuating anode rod is greater than the set threshold, and the predicted value of the current of 1–3 non-fluctuating anode rods in the area is greater than the set threshold  $\alpha$ ;

III: The predicted value of the current of the fluctuating anode rod is greater than the set threshold, and the predicted value of the current of the 4–7 non-fluctuating anode rods in the area is greater than the set threshold  $\alpha$ . It is shown in Figure 7.

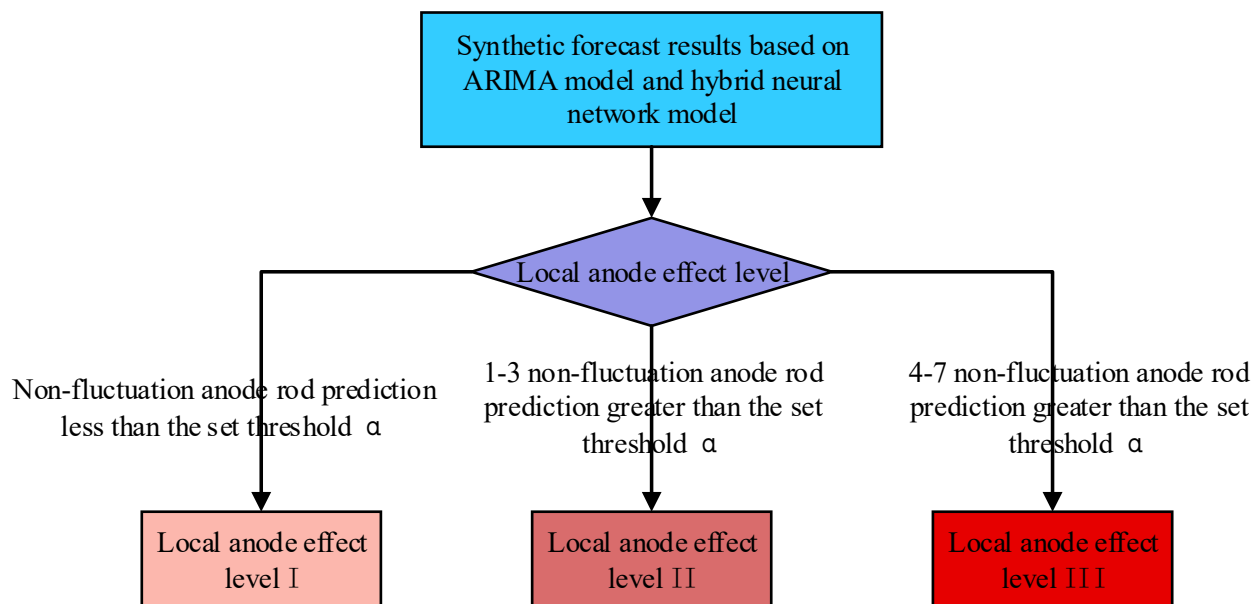
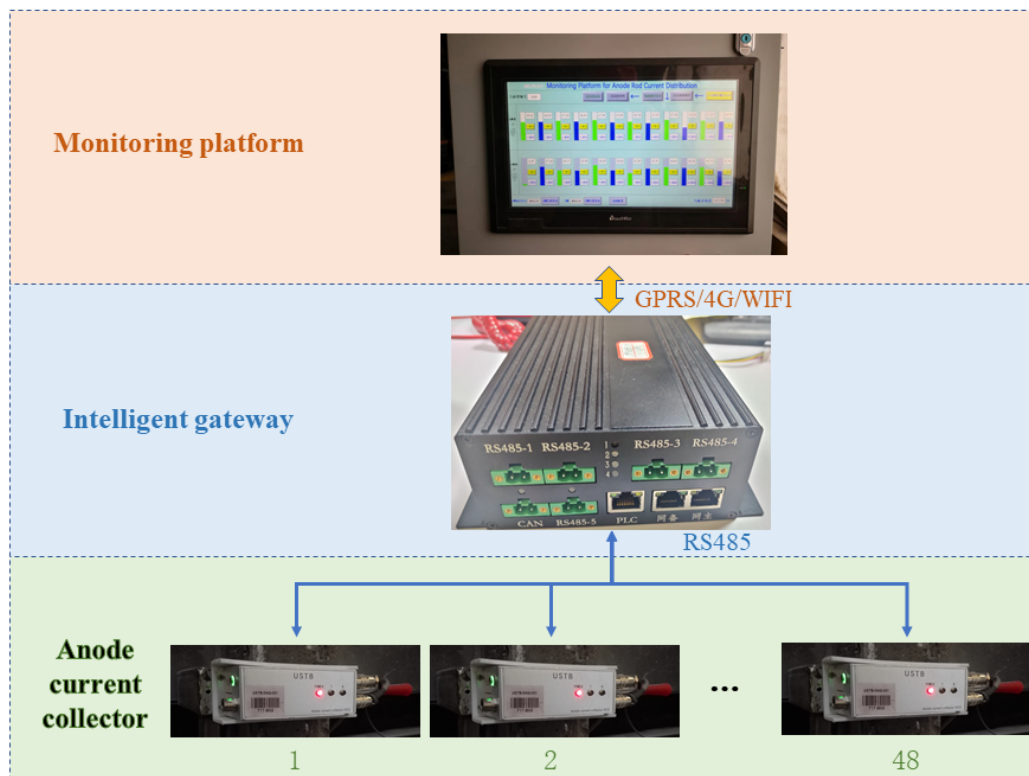


Figure 7. Levels of local anode effect.

### 5. Experimental Verification

#### 5.1. Data Acquisition

To predict the local anode effect, it is necessary to obtain the current data of aluminum electrolysis anode rod. The research group has designed a distributed anode current monitoring system for aluminum reduction cell for data acquisition, transmission, storage, and display. The system block diagram is shown in Figure 8. The anode current collector can collect the anode current in real time and monitor the ambient temperature in real time to ensure its good operating conditions, and it supports RS-485 communication. Each aluminum reduction cell contains 48 anode rods, and each anode rod is equipped with an anode current collector, which can monitor the current of each anode rods in real time. The intelligent gateway is the core part of the whole system, on the one hand, it receives and processes the instructions issued by the monitoring platform, coordinates each collector to complete the data collection, on the other hand, collects and stores the data collected by each collector and uploads it to the monitoring platform for real-time display. At the same time, the intelligent gateway has the function of interface conversion, and supports GPRS, 4G, WIFI, RS-485 and other communication methods. The monitoring platform is a man-machine interaction platform, which modifies the measurement parameters and receives the data sent by the intelligent gateway and displays them on the screen of the electric control cabinet. After many improvements and long-term debugging, it has been running stably for half a year in an electrolytic aluminum plant in southwest China, with good monitoring effect. The anode current collector takes into account the inherent noise of the circuit and external interference noise. After calibration, the measurement error in the actual field is 1.4% ~ 3.2%.



**Figure 8.** Block diagram of distributed anode rod current monitoring system for aluminum reduction Cells.

Nine groups of global anode effect data of #2832 aluminum reduction cell were collected from 27 September 2020 to 1 April 2021, including the occurrence time, and anode rod current data 40 min before and 20 min after the occurrence. The occurrence time of anode effect is shown in Table 1, where the local anode effect area and the position of fluctuating anode rod are determined by current fluctuation detection.

**Table 1.** 9 groups of anode effect data.

Number	Area	AE Time	Position
1	Area1	27 September 2020/13:25:15	B3
2	Area3	15 October 2020/16:14:30	A12
3	Area6	3 November 2020/8:34:16	B22
4	Area1	25 November 2020/18:28:45	A2
5	Area4	6 December 2020/11:13:15	A15
6	Area2	3 January 2021/13:25:32	B6
7	Area4	12 February 2021/14:33:15	B14
8	Area5	18 February 2021/19:41:15	A19
9	Area1	15 March 2021/06:25:15	A2

### 5.2. Simulation Experiment

LSTM, Convolutional Neural Network-Long Short-Term Memory (CNN-LSTM) and improved GRU-LSTM hybrid neural networks are respectively used to track and predict the current of fluctuating anode rods in each area, and determine the predictive value of the occurrence time of anode effect. As can be seen from the third part of the paper, the whole aluminum reduction cell is divided into six areas, and in order to compare the fluctuation of current prediction in each area, a fluctuating anode rod is selected in each region for current tracking prediction. In order to compare the differences between several methods more clearly, a local zoomed-in view of the prediction results is pointed out with arrows in the figure. The predicted results of anode rod current fluctuation are shown in Figure 9.

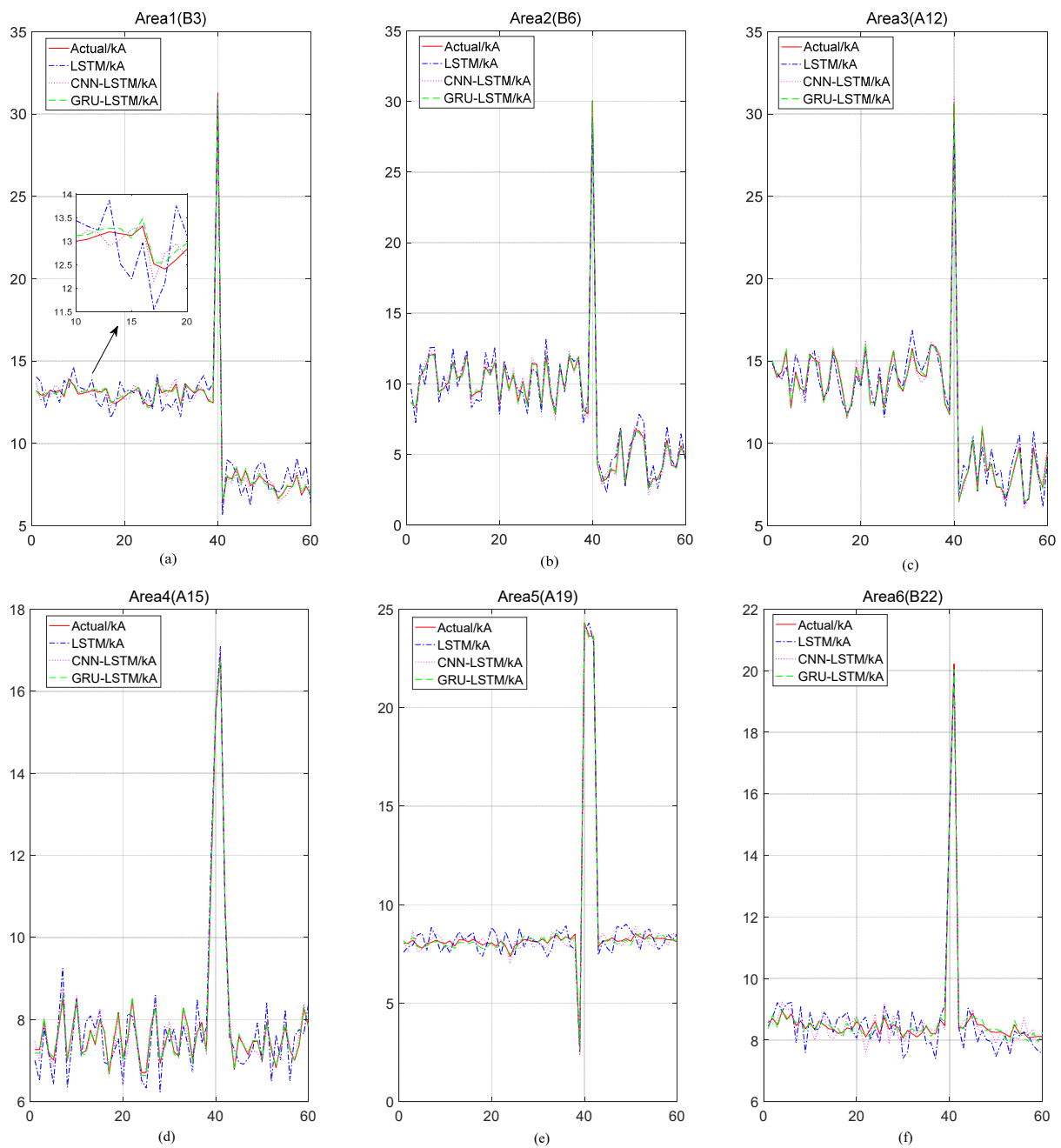


**Figure 9.** Prediction diagram of fluctuating current in 6 areas of aluminum reduction cell.

According to the comparison of the three methods in subfigures a–f, the prediction curves of GRU-LSTM hybrid neural networks are closer to the actual current fluctuation in each area of the aluminum reduction cell. In addition, the enlarged area guided by the arrow in Figure 9a can be reflected more clearly. After testing, the time set to 50 rounds of training is reduced to 2.4 s, and this is quicker than another two methods. Taking area 1 as an example, the prediction time is analyzed. According to the current prediction results of fluctuating anode rods B3 in area 1 in Figure 9a, the ARIMA model is used to predict the current of seven non-fluctuating anode rods in area 1. The current prediction of eight anode rods in area 1 is shown in Figure 10.

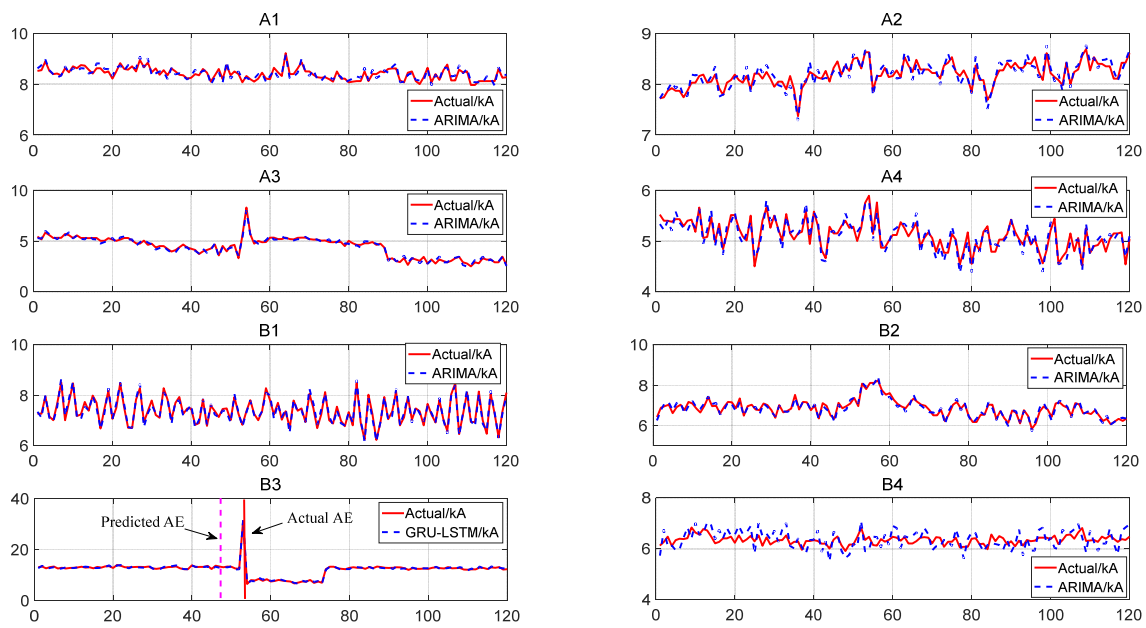


Figure 10. Area 1 anode rod current fluctuation diagram.

Figure 10(A1) shows the comparison between the actual current situation of A1 anode rod in region 1 and the results predicted by ARIMA model. Figure 10(A2–A4,B1–B4) indicate the same meaning. It can be seen from Figure 10 that the ARIMA model can effectively predict the current of non-fluctuating anode rod, with consistent prediction trend and small prediction error. Combined with the prediction results of fluctuating anode rod current, the prediction time of anode effect can be advanced to 5–10 min.

In order to quantify the prediction results, Table 2 shows the mean absolute error (MAE) and mean square error (MSE) of the prediction results of the three methods in six areas of the aluminum reduction cell.

Table 2. 6 areas MAE, MSE of three models.

Area	Model	MAE	MSE
Area1	LSTM	1.2834	10.7425
	CNN-LSTM	1.6688	7.2261
	GRU-LSTM	0.7674	5.3984
Area2	LSTM	1.7317	11.0440
	CNN-LSTM	1.0992	7.7306
	GRU-LSTM	0.6360	4.9796
Area3	LSTM	2.3139	10.5886
	CNN-LSTM	2.1652	7.1304
	GRU-LSTM	0.7543	5.2048
Area4	LSTM	1.3038	11.4501
	CNN-LSTM	1.6883	7.4859
	GRU-LSTM	1.0851	5.2771
Area5	LSTM	2.0312	11.7961
	CNN-LSTM	1.7280	7.9029
	GRU-LSTM	0.6182	5.4486
Area6	LSTM	1.5773	10.2655
	CNN-LSTM	1.8256	7.1738
	GRU-LSTM	0.4752	5.1290

It can be seen from Table 2 that compared with LSTM and CNN-LSTM networks, the MAE of GRU-LSTM network is reduced by 0.9014 and 0.5162 on average, and the MSE is



reduced by 5.344 and 2.128 on average, and the prediction results of fluctuating anode rod current in six areas are more accurate.

According to the criteria for determining the anode effect level proposed in this paper, the local anode effect level of nine groups of anode effects is shown in Table 3, which is basically consistent with the industrial field conditions.

**Table 3.** Local anode effect level.

Number	Area	N	Level
1	Area1	0	I
2	Area3	5	III
3	Area6	3	II
4	Area1	2	II
5	Area4	1	II
6	Area2	6	III
7	Area4	2	II
8	Area5	7	III
9	Area1	2	II

## 6. Conclusions

A local anode effect prediction method is proposed through the study of the fluctuation detection and prediction of anode rod current. The fluctuation of real-time current is monitored using the density test method with time-sliding window, and the improved GRU-LSTM neural network model and ARIMA algorithm are used to predict the current of fluctuating and non-fluctuating anode rod, respectively. A local anode effect level strategy based on the anode rod current prediction is proposed from the mechanism of local anode effect occurrence. Thus, we can better detect different anode rods current conditions and more accurately predict the arrival time and level of the anode effect, so that we can be more fully prepared for the appearance of the anode effect or have more sufficient time to take corresponding measures to avoid the occurrence of the anode effect. Simulation experiments based on actual industrial aluminum plant data advance the local anode effect prediction time to 5–10 min. Compared with LSTM and CNN-LSTM networks, the GRU-LSTM network is more accurate in predicting anode current and can effectively predict the occurrence of anode effect. The research in this paper is based on the anode effect prediction problem in large-scale aluminum electrolytic cells, which provides another new option for solving the anode effect prediction problem and lays the foundation for future research on active anode effect extinction work. It contributes to the smooth operation of aluminum electrolytic cells, green operation, and reduction of resource waste.

**Author Contributions:** Conceptualization, J.C. and Q.L.; methodology, Z.L. and B.L.; software, Z.L.; validation, Q.Y., R.H. and H.L.; formal analysis, J.C. and X.L.; investigation, B.L. and X.L.; resources, Q.L. and B.C.; data curation, J.C., R.H. and X.L.; writing—original draft preparation, B.L.; writing—review and editing, J.C. and Z.L.; visualization, Z.L. and J.C.; supervision, Q.L. and Q.Y.; project administration, H.L. and B.C.; funding acquisition, J.C. and Q.L. All authors have read and agreed to the published version of the manuscript.

**Funding:** This research was funded by the China Postdoctoral Science Foundation, grant number 2021M690798; Guizhou Province Science and Technology Plan Project, grant number [2021] General 085; National Natural Science Foundation of China, grant number 62273033; Chinese Society of Academic Degrees and Graduate Education, grant number 2020MSA117.

**Institutional Review Board Statement:** Not applicable.

**Informed Consent Statement:** Not applicable.

**Data Availability Statement:** Not applicable.

**Conflicts of Interest:** The authors declare no conflict of interest.

## References

1. Liu, Y.X.; Li, J. *Modern Aluminum Electrolysis*; Metallurgical Industry Press: Beijing, China, 2008.
2. Li, J.; Ding, F.Q.; Li, M.J.; Xiao, J.; Zou, Z. Intelligent anode effect prediction method for prebaked-anode aluminum reduction cells. *J. Cent. South Univ. Technol. (Nat. Sci.)* **2001**, *32*, 29–32.
3. Xiao, G.Q.; Yin, Y.X.; Cui, J.R.; Wang, J.Q.; Zhang, S. Feature Extraction of Anode Effect Based on Digital Filter and Local Mean Decomposition. In Proceedings of the 2016 IEEE 7th International Conference on Software Engineering and Service Science (ICSESS), Beijing, China, 26–28 August 2016; pp. 893–897.
4. Zhou, K.B.; Yu, D.Z.; Cao, B.; Guo, S.H.; Wang, Z.Q.; Lin, Z.K. Research of Anode Effect Prediction of Aluminum Electrolysis Cell Based on Generalized Regression Neural Network. *Control Eng. China* **2017**, *24*, 1756–1762.
5. Yang, C.; Zhou, L.; Huang, K.; Ji, H.; Long, C.; Chen, X.; Xie, Y. Multimode process monitoring based on robust dictionary learning with application to aluminum electrolysis process. *Neurocomputing* **2019**, *332*, 305–319. [[CrossRef](#)]
6. Huang, K.K.; Wen, H.F.; Ji, H.Q.; Cen, L.H.; Chen, X.F.; Yang, C.H. Nonlinear process monitoring using kernel dictionary learning with application to aluminum electrolysis process. *Control Eng. Pract.* **2019**, *89*, 94–102.
7. Li, Q.C.; Pan, H.; Cheng, X.R. Anode effect prediction method based on improved cross entropy algorithm. *Foreign Electron. Meas. Technol.* **2019**, *38*, 142–146.
8. Yin, G.; Chen, G.; He, W.; Yan, F.Y.; Luo, B.; Li, R. Anode effect prediction of 300 kA aluminum electrolysis cell based on deep learning. *Chin. J. Nonferrous Met.* **2021**, *31*, 161–170.
9. Gui, W.H.; Yue, W.C.; Xie, Y.F.; Zhang, H.L.; Yang, C.H. A Review of Intelligent Optimal Manufacturing for Aluminum Reduction Production. *Acta Autom. Sin.* **2018**, *44*, 1957–1970.
10. Ding, P.L. *Simulation Study of Alumina Concentration and Electrolyte Temperature Field under Feeding Process in the Aluminum Reduction Cell*; Huazhong University of Science & Technology Wuhan: Wuhan, China, 2016.
11. Wong, D.S.; Tabereaux, A.; Lavoie, P. Anode Effect Phenomena during Conventional AEs, Low Voltage Propagating AEs & Non-Propagating AEs. In *Light Metals 2014*; Springer: Cham, Switzerland, 2014; pp. 529–534.
12. Viumdal, H.; Mylvaganam, S.; Ruscio, D.D. System Identification of a Non-Uniformly Sampled Multi-Rate System in Aluminum Electrolysis Cells. *Model. Identif. Control* **2014**, *35*, 127–146.
13. Zhang, H.L.; Guo, H.; Li, J.; Yang, S.; Zhou, Z.; Chen, X.F.; Xie, Y.F. Industrial experiments of single point feeding control method in Large-scale aluminum reduction cell. *IFAC-Pap. OnLine* **2018**, *51*, 179–182. [[CrossRef](#)]
14. Cui, J.R.; Zhang, S.; Cao, B.; Li, Q.; Huang, R.Y.; Yang, X. Anode effect prediction method based on local effect detection. In Proceedings of the Chinese Automation Congress (CAC), Shanghai, China, 6–8 November 2020; pp. 4718–4722.
15. Yang, S.; Zhang, H.L.; Zou, Z.; Li, J.; Zhong, X.C. Reducing PFCs with Local Anode Effect Detection and Independently Controlled Feeders in Aluminum Reduction Cells. *JOM* **2020**, *72*, 229–238. [[CrossRef](#)]
16. Wang, J.Q.; Yin, Y.X.; Zhang, L.; Xiao, G.Q.; Cui, J.R.; Zhang, S. Online Monitoring System of Alumina Concentration in Aluminum Electrolytic Cell. In Proceedings of the IEEE International Conference on Information and Automation (ICIA), Ningbo, China, 1–3 August 2016; pp. 1100–1104.
17. Dion, L.; Gaboury, S.; Kiss, L.I.; Poncsak, S.; Lagace, C.L. New Approach for Quantification of Perfluorocarbons Resulting from High Voltage Anode Effects. In Proceedings of the TMS Annual Meeting & Exhibition, Phoenix, AZ, USA, 11–15 March 2018; Springer: Cham, Switzerland, 2018; pp. 1469–1477.
18. Dion, L.; Kiss, L.I.; Poncsak, S.; Lagace, C.L. Simulator of Non-homogenous Alumina and Current Distribution in an Aluminum Electrolysis Cell to Predict Low-Voltage Anode Effects. *Metall. Mater. Trans. B* **2018**, *49*, 737–755.
19. Andreev, O.N.; Slavutskiy, A.L.; Slavutskii, L.A. Neural network in a “sliding window” for power grids signals structural analysis. *IOP Conf. Ser. Earth Environ. Sci.* **2022**, *990*, 012054.
20. Pan, H.; Kong, L.; Chen, X.R.; Zhou, K.B.; Liu, J.; Xu, Q. A modified neighborhood mutual information and light gradient boosting machine-based long-term prediction approach for anode effect. *Meas. Sci. Technol.* **2019**, *30*, 115105.
21. Wang, J.F.; Jia, Y.; Wang, D.B.; Xiao, W.J.; Wang, Z.F. Weighted IForest and Siamese GRU on Small Sample Anomaly Detection in Healthcare. *Comput. Methods Programs Biomed.* **2022**, *218*, 106706. [[CrossRef](#)] [[PubMed](#)]
22. Zhou, K.B.; Zhang, Z.X.; Liu, J.; Hu, Z.X.; Duan, X.K.; Xu, Q. Anode effect prediction based on a singular value thresholding and extreme gradient boosting approach. *Meas. Sci. Technol.* **2018**, *30*, 015104. [[CrossRef](#)]
23. Liu, H.; Tian, H.Q.; Li, Y.F. Comparison of two new ARIMA-ANN and ARIMA-Kalman hybrid methods for wind speed prediction. *Appl. Energy* **2012**, *98*, 415–424.